


# Contribution of a distal radioulnar joint stabilizer on forearm stability: A modeling study

Batbayar Khuyagbaatar<sup>1,2</sup>, Sang-Jin Lee<sup>3</sup>, Ulziikhutag Bayarjargal<sup>4</sup>, Maro Cheon<sup>1</sup>, Temuujin Batbayar<sup>1</sup> and Yoon Hyuk Kim<sup>1,5</sup> 

Proc IMechE Part H:  
*J Engineering in Medicine*  
1–8  
© IMechE 2021  
Article reuse guidelines:  
sagepub.com/journals-permissions  
DOI: 10.1177/09544119211011334  
journals.sagepub.com/home/pih  


## Abstract

Instability of the forearm is a complex problem that leads to pain and limited motions. Up to this time, no universal consensus has yet been reached as regards the optimal treatment for forearm instability. In some cases, conservative treatments are recommended for forearm instability injuries. However, quantitative studies on the conservative treatment of forearm instability are lacking. The present study developed a finite element model of the forearm to investigate the contribution of the distal radioulnar joint stabilizer on forearm stability. The stabilizer was designed to provide stability between the radius and ulna. The forearm model with and without the stabilizer was tested using the pure transverse separation and radial pull test for the different ligament sectioned models. The percentage contribution of the stabilizer and ligament structures resisting the load on the forearm was estimated. For the transverse stability of the forearm, the central band resisted approximately 50% of the total transverse load. In the longitudinal instability, the interosseous membrane resisted approximately 70% of the axial load. With the stabilizer, models showed that the stabilizer provided the transverse stability and resisted almost 1/4 of the total transverse load in the ligament sectioned models. The stabilizer provided transverse stability and reduced the loading on the ligaments. We suggested that a stabilizer can be applied in the conservative management of patients who do not have the gross longitudinal instability with the interosseous membrane and the triangular fibrocartilage complex disruption.

## Keywords

Stabilizer, distal radioulnar joint, forearm instability, ligament injury, biomechanics

Date received: 15 December 2019; accepted: 29 March 2021

## Introduction

Instability of the forearm is a complex problem that disrupts the main stabilizer of the radius and ulna, which leads to pain and limited motion.<sup>1</sup> The primary contributor to longitudinal forearm stability is the radial head (RH), and the secondary stabilizers are the triangular fibrocartilage complex (TFCC) and the interosseous membrane (IOM).<sup>2,3</sup> Longitudinal forearm instability occurs when a traumatic axial load is transmitted from the wrist to the elbow because of falling or an outstretched hand that causes an RH fracture, a disruption of the distal radioulnar joint (DRUJ), and rupture of the IOM.<sup>1,4</sup> With respect to transverse forearm instability, the IOM is the main structure providing the stability by connecting the radius and ulna with a strong ligamentous band. The annular ligament also provides some stability.<sup>5–7</sup> Pfaeffle et al.<sup>5</sup> first explored that the function of the IOM is to keep the radius and ulna from

splaying apart. A traumatic dislocation of the RH is an example of the transverse instability of the forearm, which can occur with and without any bone injury.<sup>6</sup>

<sup>1</sup>Department of Mechanical Engineering, Kyung Hee University, Yongin, Korea

<sup>2</sup>Biomechanical research laboratory, Department of Technical Mechanics, School of Mechanical Engineering and Transportation, Mongolian University of Science and Technology, Ulaanbaatar, Mongolia

<sup>3</sup>Department of Orthopaedics, Seoul Bonbridge Hospital, Seoul, Korea

<sup>4</sup>Department of Electronic Engineering, College of Electronics and Information, Kyung Hee University, Yongin, Korea

<sup>5</sup>Integrated Education Institute for Frontier Science & Technology (BK21 four), Kyung Hee University, Yongin, Korea

### Corresponding author:

Yoon Hyuk Kim, Department of Mechanical Engineering, Kyung Hee University, 1732, Deogyong-daero, Giheung-gu, Yongin-si, Gyeonggi-do 17104, Korea.

Email: yoonhkim@khu.ac.kr

Clinical examination and radiographs are obtained to diagnose forearm injuries related to the instability. The injury to the IOM can be detected with magnetic resonance imaging and ultrasound.<sup>8–10</sup> In patients with gross radioulnar instability associated with RH fractures, the “radius pull test” can be used to assess signs of IOM and TFCC disruption.<sup>2</sup> Once the diagnosis is established, various surgical treatments can be used to treat forearm instability, ranging from a repair of the IOM or the TFCC, RH replacement, or ligament reconstructions.<sup>1,3,11</sup> IOM reconstruction with a bone-patellar tendon-bone graft,<sup>12</sup> semitendinosus tendon,<sup>13</sup> palmaris longus tendon or flexor carpi radialis tendon,<sup>14</sup> and mini-TightRope<sup>15</sup> are described. Arthroscopic repair of the TFCC can be performed using polydioxanone sutures.<sup>16</sup> Chronic injury with RH fracture requires RH excision and prosthetic replacement.<sup>4</sup> Up to this time, no universal consensus has yet been reached as regards the optimal treatment for forearm instability injury.<sup>3</sup> In some cases, conservative treatments are recommended and proposed to stabilize the wrist and forearm instability injuries using a brace or orthosis fabrication.<sup>17–22</sup> Millard et al.<sup>17</sup> showed that the use of a stabilizer may help in reducing the motion of the radius and ulna. O’Brien and Thurn<sup>19</sup> used an orthosis to treat patients with wrist instability. The functional brace was also used for a nonoperative treatment of residual pain following DRUJ surgery.<sup>21</sup> However, quantitative studies on the conservative treatment of forearm instability are lacking.

Computational models have been increasingly used as a biomechanical tool to quantitatively evaluate joint behavior, instability, and prosthetic replacements of the wrist, elbow, and forearm for various scenarios in advance to clinical and experimental studies.<sup>23–31</sup> The upper extremity models are mainly formulated using rigid body modeling (RBM), and highly efficient for kinematic analysis when the material deformations are not considered.<sup>23–26,30</sup> Spratley and Wayne<sup>24</sup> simulated injury models to create the varus instability of the forearm. Rahman et al.<sup>26</sup> examined the effects of ligament sectioning on elbow joint characteristics. While finite element (FE) analysis is necessary when quantifying the stress/strain in the structures as well as investigating the interaction between the musculoskeletal models with deformable bodies.<sup>31</sup> Rahman et al.<sup>26</sup> developed the elbow FE model for predicting the joint compression and contact area. The strains in the intact and implanted humerus and ulna bones were also simulated via FE analysis.<sup>29</sup> However, there are a limited number of studies that have focused on the non-surgical treatment of forearm instability. In addition to understanding the computational modeling, the complex rigid body modeling with deformable bodies can solve through the FEA. Therefore, we developed a three-dimensional (3D) FE model of the forearm to investigate the contribution of the DRUJ stabilizer on forearm stability based on a previously validated model.<sup>32</sup>

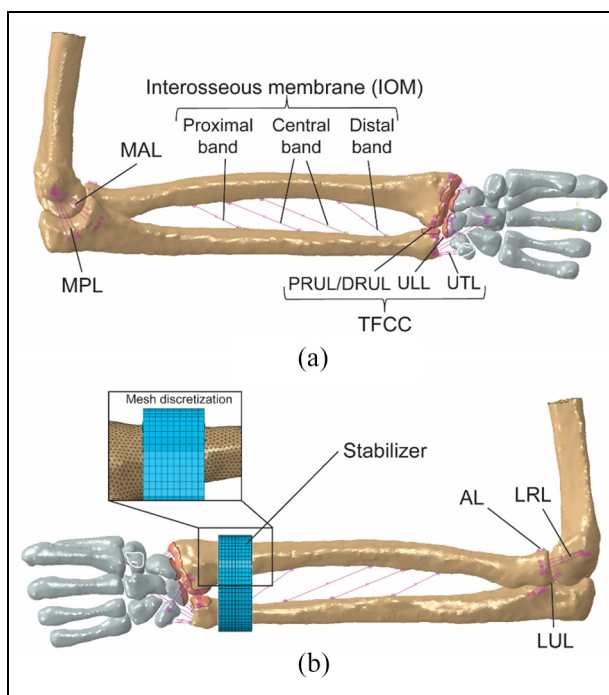


**Figure 1.** Forearm model in the: (a) palmar and (b) dorsal views without and with a DRUJ stabilizer.

We hypothesized that the stabilizer will provide either transverse or longitudinal stability of the forearm.

## Methods

### Development of the forearm model

The 3D finite element model of the forearm was developed based on our previously validated model using ABAQUS/Standard software (ABAQUS<sup>TM</sup>, ABAQUS Inc., Providence, RI, USA).<sup>32</sup> The model includes a total of 16 bones (i.e. humerus, radius, ulna, pisiform, triquetrum, lunate, scaphoid, trapezium, trapezoid, capitate, hamate, and five metacarpal bones) and 16 ligaments (represented by 38 linear spring elements) (Figure 1). Bone geometry was reconstructed from 1 mm computed tomography (CT) scans with a pixel size of 0.822 mm of a male (21 years, 1.7 m in height, 65 kg in weight) provided by the Digital Korean Project (<http://dk.kisti.re.kr>). Although both MRI and CT imaging can be used for model development,<sup>26</sup> most of the studies have been utilized CT images.<sup>23–25,27–30</sup> An average element size of 1.5 mm was used for tetrahedral elements, whereas an average element size of 2 mm was used for hexahedral elements as similar to the previous study.<sup>31</sup> The forearm model had 389,581 elements, whereas the stabilizer had 9145 elements. Surface-to-surface contact discretization was applied to the humeroulnar joint, humeroradial joint, proximal radioulnar joint, DRUJ, and radiocarpal joints, where the contact was considered frictionless.<sup>23</sup> All bones were considered a rigid body; the effect of stiffness of the bone and

**Table 1.** Ligament properties used in the forearm model.<sup>25,28</sup>

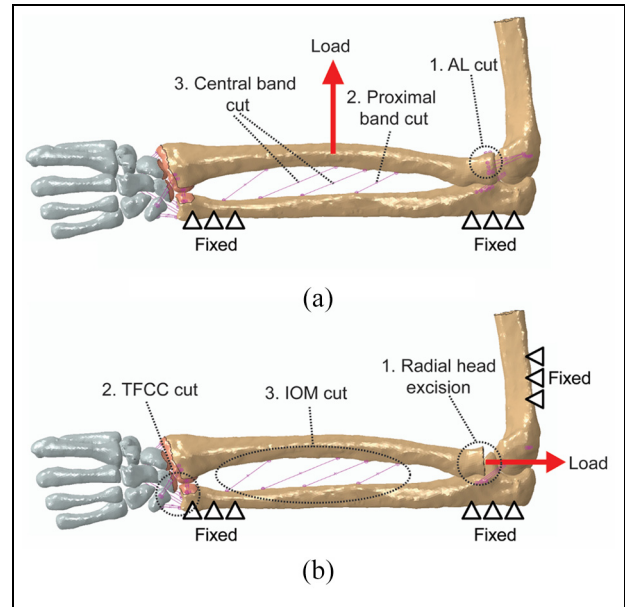
Ligament name	Abbreviation	Stiffness (N/mm)
Long radiolunate	LRL	40.0
Short radiolunate	SRLL	40.0
Radiocapitate	RCL	50.0
Radioscaphoid	RSL	50.0
Ulnocapitate	UCL	50.0
Ulnolunate	ULL	40.0
Ulnotriquetral	UTL	40.0
Dorsal radiocarpal	DRCL	75.0
Dorsal radioulnar	DRUL	13.2
Palmar radioulnar	PRUL	11.0
Medial anterior	MAL	72.3
Medial posterior	MPL	52.2
Lateral radial	LRL	15.5
Lateral ulnar	LUL	57.0
Annular	AL	28.5
Interosseous membrane		
Distal/proximal band	DB/PB	18.9
Central band	CB	65.0

cartilage had little effect on contact stresses and predicted contact areas.<sup>28</sup> The cartilage was not considered since the cartilage thickness is small in the wrist.<sup>23</sup> The ligaments were modeled as two or more tension-only spring elements. The origin and insertion points of the ligaments were described as point-to-point contact and identified based on previously published studies.<sup>23,25,26</sup> Table 1 presents the details of the ligament and stiffness coefficients. The TFCC was represented by the dorsal (DRUL) and palmar radioulnar ligaments (PRUL), ulnolunate ligament (ULL), and ulnotriquetral ligament (UTL).<sup>16</sup> The IOM was composed of a proximal band (PB), distal band (DB), and central band (CB).<sup>11</sup>

### Model validation

Two different tests were performed to validate the model. The first validation was to replicate the “pure transverse separation test” described in a study by Anderson et al.<sup>6</sup> They applied a transverse force of 150 N to displace the radius in a radial direction away from the ulna and approximately 3 mm of translation was recorded. The experiments were conducted with sequential sectioning of the ligaments, where the annular ligaments (AL) were first sectioned, followed by PB and CB of the IOM. In this study, a transverse displacement of 3 mm was applied to the radius for the intact and ligament sectioned models according to the cadaver study (Figure 2(a)).<sup>6</sup> The ulna was fixed, and the radius was able to move only in the transverse direction. The resistance forces were measured for different models and compared with the cadaver experimental study.<sup>6</sup>

A second validation was performed to reproduce the “radius pull test” designed to indicate the longitudinal instability of the forearm by measuring the radial migration after sectioning the TFCC and the IOM.<sup>2</sup>

**Figure 2.** Model descriptions for the: (a) pure transverse separation and (b) radius pull tests.

The RH was excised, and the ulna and humerus were fixed with the elbow in 90° flexion. An 89.2 N load was applied to the proximal part of the radius to displace the radius away from the radiocarpal joints representing a 9.1 kg weight loaded in the cadaver study (Figure 2(b)).<sup>2</sup> The simulation was performed after RH resection, after each sectioning of the TFCC and IOM, and after sectioning of both of TFCC and IOM. The measured radial migrations were compared to those obtained in the cadaver study.<sup>2</sup>

### Stabilizer placement

The stabilizer was designed to provide stability between the radius and ulna and placed around the DRUJ (Figure 1(b)).<sup>32</sup> Stabilizer geometry was simplified as a wrist band with width and thickness of 20 and 4 mm, respectively. The stabilizer was a thermoplastic elastomer material with an elastic modulus of 168 MPa and a Poisson’s ratio of 0.4.<sup>33</sup> The space between the stabilizer and the bones were filled with a soft material representing the skin tissue, where the tied contact was generated. The elastic modulus of the skin tissue was 0.21 MPa based on a previous study.<sup>34</sup>

### Pure transverse separation test

The forearm model with and without the stabilizer was tested using the pure transverse separation test for the intact and ligament sectioned models described earlier in the first validation (Figure 2(a)). In the previous experiment study, a force of 150 N was used in the transverse separation test.<sup>6</sup> Therefore, loads of 75, 150, and 225 N were applied to the radius in a radial direction away from the ulna. The transverse displacements

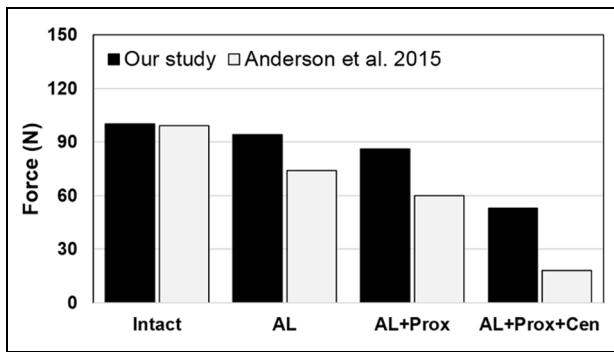


**Figure 3.** Measured transverse forces in our model and in the experimental study.

of the radius were measured for each case. The ligaments were sectioned as follows: AL was sectioned first, followed by PB and CB.

The percentage contribution of the AL, PB, CB, and remaining structure resisting the transverse separation test with and without the stabilizer was simultaneously analyzed. A 6 mm displacement was applied to the radius, and the total reaction force was recorded. Stuart et al.<sup>35</sup> described a displacement control method to evaluate the percentage contribution of each ligament in resisting transverse separation of the radius and ulna, where they used a maximum displacement of 6 mm in the testing. The resultant decrease in the reaction force reflects the relative contribution of the ligament structure to the total reaction force as each ligament was sectioned.<sup>6</sup> The strains in the DRUL and the DB were then measured.

### Radius pull test

Similarly, the forearm model with and without the stabilizer was tested using the radius pull test for the intact and ligament sectioned models described earlier in the second validation (Figure 2(b)). Loads of 44, 89, and 133 N were applied to the proximal part of the radius. The radial migrations were measured after an RH resection and then after TFCC and IOM sectioning.

Accordingly, 6 mm of the proximal radial migration was reproduced based on the cadaver study to calculate the percentage contribution of the TFCC, IOM, and the remaining structures resisting the longitudinal force.<sup>2</sup> A forearm instability higher than 6 mm indicated the gross longitudinal instability with a disruption of all of the ligamentous structures of the forearm.

## Results

### Model validation

The predicted forces resisting the transverse separation test for the intact and injured models were compared with those of the previous cadaver study (Figure 3).<sup>6</sup>

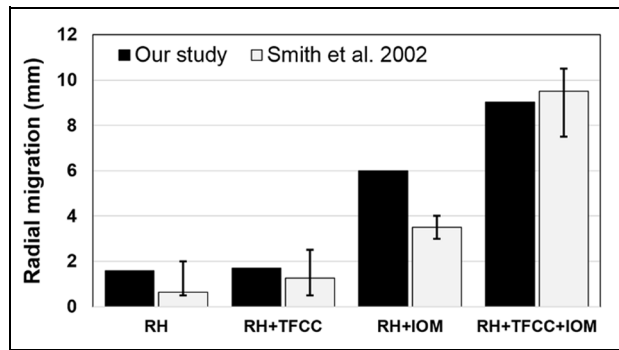


**Figure 4.** Radial migration in our model and in the experimental study.

The predicted forces were 100, 94, 86, and 53 N for the intact models after AL sectioning, PB (AL + PB) resectioning, and CB (AL + PB + CB) resectioning, respectively. The results showed a similar trend to the experimental results, although slightly higher values were obtained in the injured models.

In the radius pull test, radial migration was compared well with the previous experimental results (Figure 4).<sup>2</sup> The radial migrations were 1.5, 1.7, 5.9, and 9.0 mm after RH resectioning, after sectioning each of the TFCC (RH + TFCC) and IOM (RH + IOM), and after sectioning both TFCC and IOM (RH + TFCC + IOM). In the experimental study, the radial migrations were 0.5–2, 0.5–2.5, 3.0–4.0, and 7.5–10.5 mm for the RH, RH + TFCC, RH + IOM, and RH + TFCC + IOM, respectively.<sup>2</sup>

### Pure transverse separation test

The transverse displacement of the radius was measured for the intact and ligament sectioned models with and without the stabilizer under 75, 150, and 225 N loads (Figure 5(a)). AL and PB sectioning had a small effect on the transverse displacement of the radius (3.7%–10.4% increases of the transverse instability), and CB sectioning resulted in greater increases in the transverse displacement (56.4%–61.4% increases of the transverse instability). After stabilizer placement, the transverse displacements were lower than those in the results from the intact model, regardless of the loads and sectioning of the ligaments.

The percentage contributions of AL, PB, CB, and the remaining structure resisting the transverse separation of the ulna and radius were 4.8%, 12.7%, 55.7%, and 26.8%, respectively (Figure 6(a)). The load on the CB was reduced by 16.1% after the stabilizer was worn. In another way, the stabilizer resisted 23.7% of the total transverse load alone. The model at a maximum load of 225 N showed that the stabilizer supported the stability in a transverse direction even in the case of AL + PB + CB. Meanwhile, the strains in the DRUL and the DB were reduced by 15%–20% (Figure 7(a)).

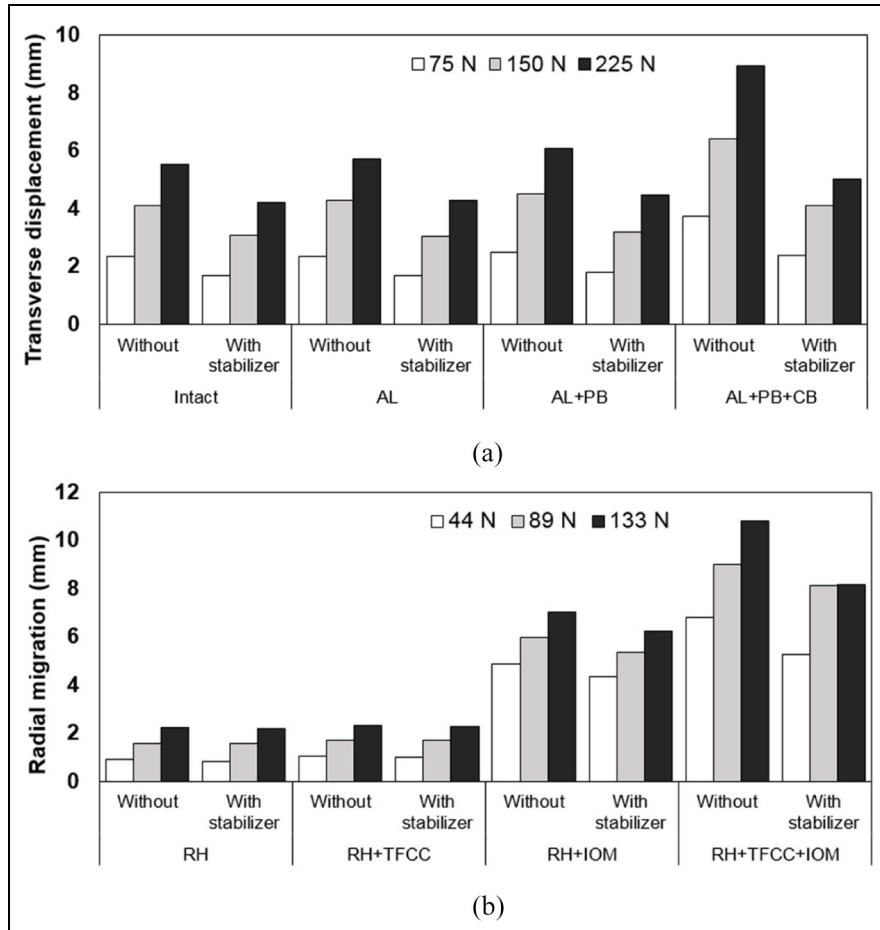


**Figure 5.** (a) Transverse displacement of the radius in the pure transverse separation test and (b) radial migration in the radius pull test for the intact and injured models with and without a stabilizer.

**Radius pull test**

Figure 5(b) shows the radial migration with and without the stabilizer for different injured models under 44–133 N loads. RH resectioning and TFCC sectioning resulted in a 2 mm radial migration at the maximum loads. The radial migrations were greatly increased by 3–5 times after IOM sectioning (RH + IOM) with TFCC (RH + TFCC + IOM). With the stabilizer, the radial migrations were slightly reduced for the RH + IOM and RH + TFCC + IOM cases, although the longitudinal instability was 2–3 times higher than that of the RH resection-only model.

The percentage contributions of the TFCC, IOM, and remaining structure resisting the longitudinal translation were 12.5%, 76.1%, and 11.4%, respectively (Figure 6(b)). The loads on the TFCC and the IOM were reduced by only 6% with the stabilizer. The actual contribution of the stabilizer on the longitudinal stability was 5.4%. The model deformation at a maximum force of 133 N showed that the stabilizer failed to support the longitudinal stability after IOM sectioning with the TFCC (Figure 7(b)). Also, the strains in the

remained ligaments were not reduced after stabilizer placement.

**Discussion**

We developed herein a forearm model to investigate the contribution of the stabilizer on the transverse and longitudinal stabilities of the forearm. The model was validated against two cadaver studies.<sup>2,6</sup> Consequently, the model was able to predict the force resisting the separation of the radius and ulna following the incremental sectioning of the ligament structures (i.e. AL, PB, and CB) and showed a similar trend with the experimental results.<sup>6</sup> Although the model results showed very similar for the intact case, the ligament sectioned models showed an increase in force. The difference most likely arose from the ligaments modeling, where we used linear tension-only elements since the precise data of the tensile behavior of the elbow ligaments are lacking.<sup>24</sup> In the second validation, the radial migration was accurately measured after RH resectioning and TFCC and IOM sectioning. The predicted radial migrations were within the range of

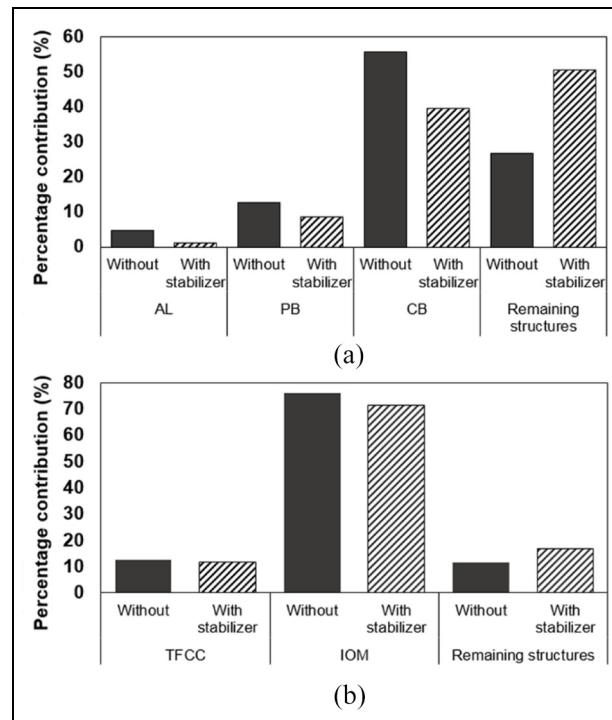


**Figure 6.** Percentage contribution of each structure in resisting the: (a) transverse and (b) longitudinal forces with and without a stabilizer.

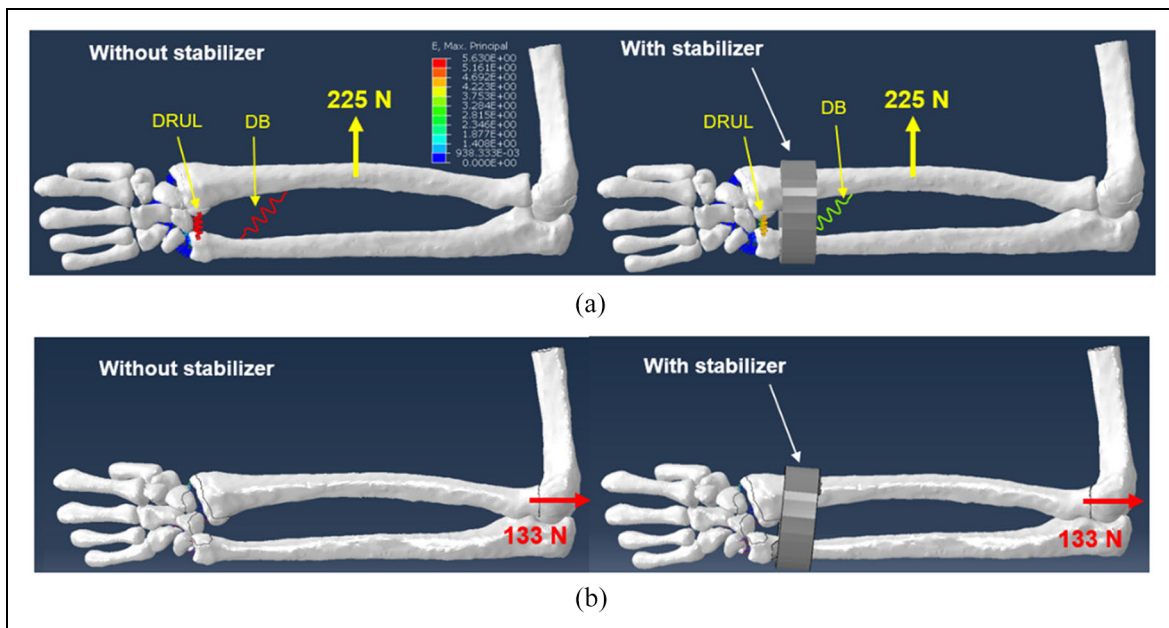


**Figure 7.** Model deformation in the: (a) pure transverse separation test and (b) radius pull test for injured models with and without a stabilizer.

the results from the experimental study.<sup>2</sup> In addition, the anatomical difference may be a reason behind the deviations observed between the studies.

The transverse and longitudinal instabilities of the forearm model were reproduced by ligament structure sectioning. The percentage contributions of each structure resisting the force through the transverse and longitudinal axes of the forearm were estimated. For the

transverse stability of the forearm, the CB resisted approximately 50% of the total transverse load to the radius. This result was similar to the experimental findings, where the percentage contribution of the CB was up to 40.3%.<sup>6</sup> In addition, the sectioning of the AL and IOM greatly increased the strains in the DRUL/PRUL as well as increased the transverse dislocation of the radius. This could be explained by an experimental

study by Werner et al.,<sup>11</sup> where they reported that increased gapping at the DRUJ when the IOM was cut, placed greater loads on the DRUL/PRUL. In the longitudinal instability, the IOM and the TFCC resisted approximately 70% and 10% of the axial load, respectively, through the hand to the elbow. Marcotte and Osterman<sup>8</sup> found that the IOM bears 71% of longitudinal stiffness, and the TFCC is responsible for 8% of the stiffness in the absence of the RH. Loeffler et al.<sup>1</sup> reported that the TFCC is responsible for 8% of the mechanical stiffness of the forearm. Moreover, the IOM was shown as an important structure in maintaining both the transverse and longitudinal stabilities of the forearm.<sup>5</sup> Furthermore, the radial migrations of 4.8–7.0 mm and 6.7–10.8 mm were observed when the IOM and IOM with TFCC ligamentous structures were cut in this study. Smith et al.<sup>2</sup> revealed that the radial migration  $\geq 3$  mm indicates an injury of IOM, while  $\geq 6$  mm is a sign of grossly unstable with an injury of IOM and TFCC.

The results showed that the stabilizer provided the transverse stability and resisted almost 1/4 of the total transverse load on the forearm. The stabilizer was modeled as an elastic band spanning the DRUJ based on a clinically available product originally developed to provide stability for the ulna and radius during sports activities. Previous studies reported that forearm or wrist braces improved the functionality of the forearm motion following injuries.<sup>17,19–21</sup> O'Brien and Thurn<sup>19</sup> successfully used a forearm orthosis in patients with wrist joint instability. Barlow<sup>20</sup> described the use of a novel brace as a non-surgical intervention for TFCC tears and showed a functional status improvement after the brace was worn. However, the stabilizer failed to provide the longitudinal stability of the forearm because the radial migration was higher than 4 mm in the cases with TFCC and IOM sectioning. The cadaver study reported that 3 mm or more of the proximal displacement of the radial head indicated ligamentous injuries in the forearm.<sup>2</sup> Also, untreated IOM damage could allow additional injury instability to the radioulnar ligaments.<sup>11</sup> However, no optimal treatment is available for the forearm longitudinal instability.<sup>3</sup> Therefore, this study suggested that a stabilizer can be applied in the conservative management of patients who do not have the gross longitudinal instability with TFCC and IOM disruption.

This study has several limitations. All bone bodies were assumed to be rigid based on previous modeling studies for computational efficiency.<sup>23,25,30</sup> The ligaments were modeled using tension-only spring elements with stiffness coefficients adopted from previous studies.<sup>23,27,30</sup> The TFCC was represented by the spring elements of PRUL, DRUL, ULL, and UTL, and the articular fibrocartilage disc and the meniscal homologue was not included in the model because they are difficult to capture by CT.<sup>23</sup> Due to this simplification, the model over-predicted the contact between the ulnar

head, triquetrum and lunate during the radius pull test. Future studies should include the TFCC structures as a soft tissue structure since it plays a major stabilizing role on the ulnar aspect of the wrist.<sup>25</sup> The stabilizer was modeled using the linear elastic property and placed around the DRUJ. Although the stabilizer geometry was simplified, the original band size was not changed in this study. The space between the bones and the stabilizer was filled with a soft material representing the skin tissue. Moreover, the transverse and longitudinal forearm instability models were simulated based on the cadaver studies.<sup>2,6</sup>

## Conclusion

The validated forearm model was used to simulate the transverse and longitudinal instabilities of the forearm. The biomechanical effects of the stabilizer on the forearm instabilities were then investigated. The model demonstrated the ability to predict the contribution of each ligamentous structure and the stabilizer resisting the force on the radius. The stabilizer provided stability during the transverse separation test and reduced the loading on the ligaments. It also particularly resisted 1/4 of the total transverse load on the forearm. However, the stabilizer failed to support the forearm during the radius pull test. Therefore, it can be used in non-surgical conservative management of patients who do not have the gross longitudinal instability of the forearm.


## Declaration of conflicting interests

The author(s) declared no potential conflicts of interest with respect to the research, authorship, and/or publication of this article.

## Funding

The author(s) disclosed receipt of the following financial support for the research, authorship, and/or publication of this article: This work was supported by the National Research Foundation of Korea (NRF) grant funded by the Korean government (MSIP) (No. 2017R1E1A1A03070418).

## ORCID iD

Yoon Hyuk Kim  <https://orcid.org/0000-0001-9127-4813>

## References

1. Loeffler BJ, Green JB and Zelouf DS. Forearm instability. *J Hand Surg* 2014; 39: 156–167.
2. Smith AM, Urbanosky LR, Castle JA, et al. Radius pull test. *The Journal of Bone and Joint Surgery-American Volume* 2002; 84: 1970–1976.
3. Adams JE. Forearm instability: anatomy, biomechanics, and treatment options. *J Hand Surg* 2017; 42: 47–52.

4. Venouziou AI, Papatheodorou LK, Weiser RW, et al. Chronic Essex-Lopresti injuries: an alternative treatment method. *J Shoulder Elbow Surg* 2014; 23: 861–866.
5. Pfaeffle HJ, Stabile KJ, Li ZM, et al. Reconstruction of the interosseous ligament unloads metallic radial head arthroplasty and the distal ulna in cadavers. *J Hand Surg* 2006; 31: 269–278.
6. Anderson A, Werner FW, Tucci ER, et al. Role of the interosseous membrane and annular ligament in stabilizing the proximal radial head. *J Shoulder Elbow Surg* 2015; 24: 1926–1933.
7. Gutowski CJ, Darvish K, Ilyas AM, et al. Interosseous ligament and transverse forearm stability: a biomechanical cadaver study. *J Hand Surg* 2017; 42: 87–95.
8. Marcotte AL and Osterman AL. Longitudinal radioulnar dissociation: identification and treatment of acute and chronic injuries. *Hand Clin* 2007; 23: 195–208.
9. Iida A, Kawamura K, Nakanishi Y, et al. A biomechanical perspective on distal radioulnar joint instability. *J Wrist Surg* 2017; 06: 088–096.
10. Daneshvar P, Willing R, Pahuta M, et al. Osseous anatomy of the distal radioulnar joint: an assessment using 3-dimensional modeling and clinical implications. *J Hand Surg* 2016; 41: 1071–1079.
11. LeVasseur M, Harley B, Anderson A, et al. Role of the Interosseous Membrane in Preventing Distal Radioulnar Gapping. *J Wrist Surg* 2016; 06: 097–101.
12. Adams JE, Culp RW and Osterman AL. Interosseous membrane reconstruction for the Essex-Lopresti injury. *J Hand Surg* 2010; 35: 129–136.
13. Soubeyrand M, Oberlin C, Dumontier C, et al. Ligamentoplasty of the forearm interosseous membrane using the semitendinosus tendon: anatomical study and surgical procedure. *Surg Radiol Anat* 2006; 28: 300–307.
14. Tejwani SG, Markolf KL and Benhaim P. Reconstruction of the interosseous membrane of the forearm with a graft substitute: a cadaveric study. *J Hand Surg* 2005; 30: 326–334.
15. Kam CC, Jones CM, Fennema JL, et al. Suture-button construct for interosseous ligament reconstruction in longitudinal radioulnar dissociations: a biomechanical study. *J Hand Surg* 2010; 35: 1626–1632.
16. Doarn MC and Wysocki RW. Acute TFCC injury. *Oper Tech Sports Med* 2016; 24: 123–125.
17. Millard GM, Budoff JE, Paravic V, et al. Functional bracing for distal radioulnar joint instability. *J Hand Surg* 2002; 27: 972–977.
18. Zimmerman RM and Jupiter JB. Instability of the distal radioulnar joint. *J Hand Surg Eur Vol* 2014; 39: 727–738.
19. O'Brien VH and Thurn J. A simple distal radioulnar joint orthosis. *J Hand Ther* 2013; 26: 287–290.
20. Barlow SJ. A Non-surgical Intervention for triangular fibrocartilage complex tears. *Physiother Res Int* 2016; 21: 271–276.
21. Boynton JF, Budoff JE and Clifford JW. The effect of forearm bracing on radioulnar impingement. *J Hand Surg* 2005; 30: 157–161.
22. Feehan L and Fraser T. Early controlled mobilization using dart-throwing motion with a twist for the conservative management of an intra-articular distal radius fracture and scapholunate ligament injury: A case report. *J Hand Ther* 2016; 29: 191–198.
23. Majors BJ and Wayne JS. Development and validation of a computational model for investigation of wrist biomechanics. *Ann Biomed Eng* 2011; 39: 2807.
24. Spratley EM and Wayne JS. Computational model of the human elbow and forearm: application to complex varus instability. *Ann Biomed Eng* 2011; 39: 1084–1091.
25. Wayne JS and Mir AQ. Application of a three-dimensional computational wrist model to proximal row carpectomy. *J Biomech Eng* 2015; 137: 061001.
26. Rahman M, Cil A, Bogener JW, et al. Lateral collateral ligament deficiency of the elbow joint: a modeling approach. *J Orthop Res* 2016; 34: 1645–1655.
27. Miguel-Andres I, Alonso-Rasgado T, Walmsley A, et al. Effect of anconeus muscle blocking on elbow kinematics: electromyographic, inertial sensors and finite element study. *Ann Biomed Eng* 2017; 45: 775–788.
28. Willing RT, Lalone EA, Shannon H, et al. Validation of a finite element model of the human elbow for determining cartilage contact mechanics. *J Biomech* 2013; 46: 1767–1771.
29. Completo A, Pereira J, Fonseca F, et al. Biomechanical analysis of total elbow replacement with unlinked iBP prosthesis: an in vitro and finite element analysis. *Clin Biomech* 2011; 26: 990–997.
30. Fisk JP and Wayne JS. Development and validation of a computational musculoskeletal model of the elbow and forearm. *Ann Biomed Eng* 2009; 37: 803–812.
31. Islam K, Duke K, Mustafy T, et al. A geometric approach to study the contact mechanisms in the patellofemoral joint of normal versus patellofemoral pain syndrome subjects. *Comput Methods Biomech Biomed Eng* 2015; 18: 391–400.
32. Khuyagbaatar B, Lee SJ, Cheon M, et al. Effect of wrist-wearing distal radioulnar joint stabilizer on distal radioulnar joint instability using a forearm finite element model. *J Mech Sci Technol* 2019; 33: 2503–2508.
33. Ausias G, Thuillier S, Omnès B, et al. Micro-mechanical model of TPE made of polypropylene and rubber waste. *Polymer* 2007; 48: 3367–3376.
34. Iivarinen JT, Korhonen RK, Julkunen P, et al. Experimental and computational analysis of soft tissue stiffness in forearm using a manual indentation device. *Med Eng Phys* 2011; 33: 1245–1253.
35. Stuart PR, Berger RA, Linscheid RL, et al. The dorso-palmar stability of the distal radioulnar joint. *J Hand Surg* 2000; 25: 689–699.